Displays 31 (2010) 196–204

Contents lists available at ScienceDirect

Displays

journal homepage: www.elsevier.com/locate/displa

Numerical comparison of LED directivity approximation functions for video displays

L. Svilainis *, V. Dumbrava

Signal Processing Department, Kaunas University of Technology, Studentu Str. 50, LT-51368 Kaunas, Lithuania

ARTICLE INFO

Article history:
Received 20 May 2010
Received in revised form 7 August 2010
Accepted 10 August 2010
Available online 25 August 2010

Keywords:
LED video displays
LED directivity approximation
Far-field pattern
Approximation error

ABSTRACT

The approximation functions of the directivity of the light emitting diodes (LED) have been investigated. LEDs used in large scale LED video displays have been studied. LED directional properties among the other parameters define the video display image quality. The simplicity of an approximation function and ease of analytical handling have been targeted. These functions suppose to be used in display directivity engineering. Four candidate approximation functions were identified and their approximation performance analyzed. The evaluation is done on eight different type LEDs' sample batches. These samples have been chosen to represent the variety of the main colors and the range of the most popular viewing angles used in large scale LED video displays design. The relative intensity approximation root mean square (RMS) error and approximation errors' cross correlation have been used as performance estimation criteria. The radiometric intensity variation within a manufacturing lot was suggested as lower error bound. Approximation error variance was analyzed for various approximation ranges. Results of four candidate approximation functions' performance on eight different type LEDs' are presented.

1. Introduction

The light emitting diode (LED) application in large scale video displays has proven a perfect tool when a large area of a high brightness imaging is required [1]. It is used to convey video information in advertising, sports, leisure or even architecture applications. LED video display is based on the raster-scanning principle: monochrome or multicolor LEDs form the image pixels. It should to be viewed at large distance: only when the neighboring pixels are observed at an angle less than 1 arc min they blend into a complete image [2]. Large LED video displays typically use small louvers to reduce the direct ambient light influence [3,4].

In order to predict the LED video display image optical performance at various viewing angles the directivity function of individual pixels' is needed. Since LEDs form the pixels then LED directional properties among the other parameters define the image quality [5,6]. The far-field pattern (FFP) [7] is used to characterize the LED spatial directivity. If the display geometry and audience placement are known then image quality can be derived through the LED directivity model. LED applications expand into complex illumination and imaging systems. Illumination system design programs can be used to design such systems [8]. However, these programs require the light source directivity model. As Cassarly et al. have indicated in [8] the model simplicity is desirable because it could be complicated to trace large numbers of rays for the each iteration of the system design. Of course, a simple model might be sufficient for a feasibility study, while a more accurate approach may be needed for the final design. Moreno et al. in [9] divide the LED models currently employed into analytical approximations or Monte Carlo ray tracing. Publication [10] proposed quite simple analytic representation for the LED FFP. Authors suggest that the final FFP is the result of the sum of three terms: the chip radiation directly refracted by the encapsulating lens, internally reflected lens walls and by the reflector cup. Mathematically, the pattern is described as the sum of a maximum of two or three Gaussian or cosine-power functions.

LEDs used in video displays have smooth directivity function with clearly expressed peak (no "batwing" or peaking). This fact led us to idea that simple approximation function might be sufficient for LED directivity estimation. Therefore the goal of this paper was to provide the comparison of simple approximation functions.

2. LED directivity

Generally FFP is obtained as the spatial intensity I distribution over the observation angles Θ (polar/zenith) and ϕ (azimuth), e.g. $I(\Theta, \phi)$. Polar angle is the inclination angle measured from the LED mechanical axis [11], according to [12] it is a line through the tip in the direction of the axis of symmetry of the body. Azimuth angle ϕ is the angle measured in plane perpendicular to mechanical axis with zero aligned with line along LED pins.

LED manufacturers specify the half power beam angle $2\Theta_{0.5}$ which is the polar angle where the intensity is half of the peak emission value. The LEDs used in video displays usually have elliptical directivity diagram, i.e. one-dimensional intensity I

* Corresponding author. Tel.: +370 37 300532; fax: +370 37 352998.
E-mail address: linas.svilainis@ktu.lt (L. Svilainis).

0141-9382/$ - see front matter © 2010 Elsevier B.V. All rights reserved.
doi:10.1016/j.displa.2010.08.001

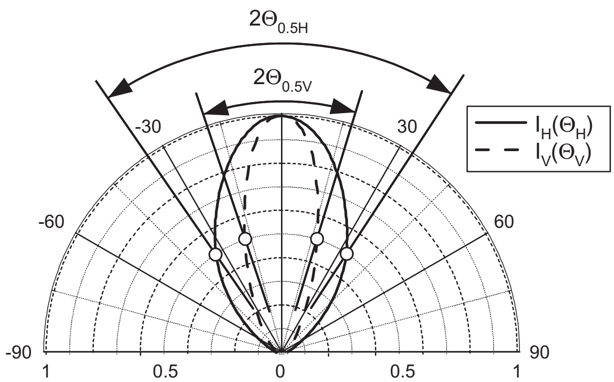

Fig. 1. LED FFP in polar coordinates.

distribution measured in vertical $I(\Theta, \phi = 0°)$ and horizontal $I(\Theta, \phi = 90°)$ plane differ (Fig. 1). The oval shape ensures wide horizontal viewing angle of display and narrow the vertical angle.

Therefore manufacturers specify two $2\Theta_{0.5}$ angles [13]: $2\Theta_{0.5H}$ measured along major axis and $2\Theta_{0.5V}$ measured along minor axis. In LED video display design it is more convenient to have a coordinate system with angles in horizontal plane and vertical plane: this will ease the audience geometry calculations. Therefore we will use angles Θ_H (Θ when $\phi = 0°$) and Θ_V (Θ when $\phi = 90°$) both having a range from $-90°$ to $90°$. Assuming the second order rotational symmetry of two-dimensional LED FFP, we limit our investigation to the one-dimensional FFPs $I_H(\Theta_H)$ and $I_V(\Theta_V)$ analysis. The two-dimensional directivity function then can be obtained as the product of last two:

$$I_{2D}(\Theta_H, \Theta_V) = I_H(\Theta_H) \cdot I_V(\Theta_V). \tag{1}$$

The amount of possible horizontal and vertical directivity angles combinations is large. The suggested split into $I_H(\Theta_H)$ and $I_V(\Theta_V)$ allows for great simplification of analysis since only one-dimensional approximation is investigated. Therefore the analysis presented below was concentrated on the one-dimensional approximation functions.

3. Candidate FFP approximation functions

The polynomial fit could be the first candidate for any approximation. Second order symmetry of the FFP was assumed. Therefore parabolic function was suggested for FFP approximation. The LED intensity I at some angle Θ is a parabolic function of a form

$$I(\Theta) = I_{\max} + a_2(\Theta - \Theta_{peak})^2, \tag{2}$$

where $I_{\max}$ is the peak intensity at Θ_{peak} angle and a_2 is a coefficient defining the FFP width. Obtaining the equation for $I(\Theta_{peak})$ and solving for a half of it, the half power beam angle $2\Theta_{0.5}$ is

$$2\Theta_{0.5} = -\frac{\sqrt{-2a_2}}{a_2}. \tag{3}$$

It was interesting to find out how higher order polynomial will behave. It was suggested to use two terms: parabolic to be responsible for peak approximation ant power of four for lower part of FFP:

$$I(\Theta) = I_{\max} + a_2(\Theta - \Theta_{peak})^2 + a_4(\Theta - \Theta_{peak})^4. \tag{4}$$

The publication [7] presents the cos in power $(g - 1)$ function as a candidate for LED FFP approximation:

$$I(\Theta) = I_{\max} \cdot \cos(\Theta - \Theta_{peak})^g, \tag{5}$$

where g is a coefficient, proportional to viewing angle $2\Theta_{0.5}$. Solving (5) for $2\Theta_{0.5}$:

$$2\Theta_{0.5} = 2\arccos(2^{\left(-\frac{1}{g}\right)}). \tag{6}$$

Gaussian approximation is most often used in LED directivity [9,10] and RF antenna pattern approximation [14] as an idealized pattern of an antenna having a smooth mainlobe with no sidelobes:

$$I(\Theta) = I_{\max} \cdot e^{\left(-\ln(2)\frac{(\Theta-\Theta_{peak})^2}{\Theta_{0.5}^2}\right)}. \tag{7}$$

Ambient light during the measurement process under some circumstances cannot be completely removed and the DC offset occurs. Then the Gaussian with DC offset I_{Off} can be used for approximation:

$$I(\Theta) = I_{Off} + I_{\max} \cdot e^{\left(-\ln(2)\frac{(\Theta-\Theta_{peak})^2}{\Theta_{0.5R}^2}\right)}. \tag{8}$$

The half power beam angle in (7) is evaluated after removing the DC component of the FFP: notation with the index $R(2\Theta_{0.5R})$ to distinguish from the conventional result. This property is useful if DC offset occurs due to the ambient light. But in case the offset is a property of LED the half power angle will have a large systematic error. Then the correct half power angle is:

$$2\Theta_{0.5} = \frac{2\Theta_{0.5R}\sqrt{-\ln\left(\frac{I_{\max}-I_{off}}{2I_{\max}}\right)}}{\sqrt{\ln(2)}}. \tag{9}$$

Above mentioned functions initial performance was presented in [15]. Moreno et al. [9] suggested multiple Gaussian terms function for LED FFP approximation. In our investigation we have included only function containing two terms:

$$I(\Theta) = I_1 \cdot e^{\left(-\frac{(\Theta-\Theta_{peak})^2}{W_1}\right)} + I_2 \cdot e^{\left(-\frac{(\Theta-\Theta_{peak})^2}{W_2}\right)}, \tag{10}$$

where W_1 and W_2 are defining the first and second term width respectively; I_1 and I_2 are weights of the terms. Further analysis was limited by aforementioned functions.

It should be noted that the selected functions are a significant simplification. Other authors are suggesting much more complicated functions: in [9] it is suggested to use:

$$I(\Theta, \phi) = \sum_i I_i \cdot e^{\left(-(\ln(2))(|\Theta|-\theta_i)^2\left(\frac{\cos^2\phi_i}{V_i}+\frac{\sin^2\phi_i}{H_i}\right)\right)}, \tag{11}$$

where Θ range is $0° \ldots 90°$ but ϕ range is $0° \ldots 360°$, angle θ_i allows for diagram offset in angular direction (useful for "batwing" patterns), coefficients V_i and H_i define the different directionality in vertical and horizontal direction and I_i is the weight assigned to ith term (usually 2–3). In [9] it was proposed that the manufacturer should include such formula with its coefficients in their technical data sheets. We support this proposal, but so far manufacturers only indicate the half power beam angle $2\Theta_{0.5H}$ measured along major axis and $2\Theta_{0.5V}$ measured along minor axis. These parameters are applicable only for simple functions like Eqs. (2), (5), and (7). We want to analyze whether much simpler approximations are powerful enough to satisfy the approximation in reduced range (slightly beyond $-\Theta_{0.5} \ldots +\Theta_{0.5}$ range) and can be applied in engineering applications like illumination rendering [16], display directivity [17] or louvers performance prediction [3,4].

4. Fitting procedure

The Matlab procedure *fminsearch*, employing the Nelder–Mead simplex method [18] have been used for fitting. The intensity approximation error root mean square (RMS) value has been used for convergence.

Table 1
Candidate functions used in investigation.

Notation	Function
Gaus	$I(\Theta) = I_{\max} \cdot e^{\left(-\ln(2)\frac{(\Theta-\Theta_{peak})^2}{\Theta_{0.5}^2}\right)}$
Gaus + offset	$I(\Theta) = I_{Off} + I_{\max} \cdot e^{\left(-\ln(2)\frac{(\Theta-\Theta_{peak})^2}{\Theta_{0.5R}^2}\right)}$
Gaus x2	$I(\Theta) = I_1 \cdot e^{\left(-\frac{(\Theta-\Theta_{peak})^2}{W_1}\right)} + I_2 \cdot e^{\left(-\frac{(\Theta-\Theta_{peak})^2}{W_2}\right)}$
$\cos^g$	$I(\Theta) = I_{\max} \cdot \cos(\Theta - \Theta_{peak})^g$
x^2	$I(\Theta) = I_{\max} + a_2(\Theta - \Theta_{peak})^2$
$x^2 + x^4$	$I(\Theta) = I_{\max} + a_2(\Theta - \Theta_{peak})^2 + a_4(\Theta - \Theta_{peak})^4$

$$e_{RMS} = \sqrt{\frac{1}{N}\sum_{i=1}^{N}(I_{orig\ i} - I_{appr}(\Theta_i))^2}, \tag{12}$$

where $I_{orig\ i}$ is the original FFP, $I_{appr}(\Theta_i)$ is the approximating function taken at the ith position of N total samples used. The best approximation accuracy was desired in high intensity region (close to peak value). Therefore Eq. (12) was additionally weighted by original FFP values

$$e_{RMSW} = \sqrt{\frac{1}{N}\sum_{i=1}^{N}\left[(I_{orig\ i} - I_{appr}(\Theta_i))^2 I_{orig\ i}\right]}. \tag{13}$$

The termination tolerance of *fminsearch* for argument and function respectively were assigned the default values, 10^{-4}, the maximum number of iteration steps was assigned four times the default value, 2000.

5. Investigation object

Variety of LED's possessing different directivity, color, and intensity exists. In this paper we analyze only LEDs dedicated for large scale video displays. The LEDs chosen for investigation represent the main colors and the range of most popular half power beam angles $2\Theta_{0.5}$. Four LED types with oval directivity diagram were chosen: Brilliance Technologies type BTL-55, Super Bright Optoelectronics type SBD-GV, LBL Photoelectric Technology type LBL-52 and Greenlight type GB70. Two one-dimensional FFPs have been measured by goniometer [19] for each LED type: $I_H(\Theta_H)$ along horizontal and $I_V(\Theta_V)$ along vertical axis. Eight resulting FFP groups were collected for analysis. The analyzed batch was taken from the same manufacturing lot. The notation used and the essential parameters are listed in Table 2.

In order to present the parameters $2\Theta_{0.5}$ and Θ_{peak} scatter, these parameters were obtained for each LED in a batch by using measured FFP. The results are presented in Table 2 (column 3 and 4) indicating the mean value and standard deviation. For majority of LEDs the angle $2\Theta_{0.5}$ obtained from original (measured) FFP is close to the manufacturer specified value.

Table 2
LEDs used for the investigation.

Notation	Specified $2\Theta_{0.5}$, °	Measured $2\Theta_{0.5}$, °	Measured Θ_{peak}, °	Color	Batch size, M
BrGH	110	106 ± 8.0	−0.7 ± 6.8	Green	20
SBORH	110	99.6 ± 3.8	1.8 ± 4.3	Red	20
Z2BH	70	70.3 ± 3.6	3.0 ± 1.7	Blue	37
GBGH	70	64.7 ± 2.1	2.4 ± 1.6	Green	20
BrGV	45	44.6 ± 1.9	2.3 ± 2.2	Green	20
Z2BV	40	43.9 ± 2.0	−0.2 ± 2.4	Blue	37
GBGV	40	35.2 ± 0.9	2.4 ± 2.0	Green	20
SBORV	45	31.3 ± 3.2	2.9 ± 1.6	Red	22

6. Performance evaluation criteria

As Cassarly has indicated in [8]: "if the scanned source is not a "typical" representative of that source type, then neither [approximation] is the model". In other words, we need some representation of ideal directivity function.

6.1. Ideal directivity approximation

For this purpose it was suggested to combine the individual LED FFP and to use the mean of multiple FFP of same type LED for "representative" FFP generation. The obtained raw data (see Fig. 2 for Z2BH results) was normalized for peak value and peak angle position moved to 0° (Fig. 3). This peak position normalization was introduced to reduce the influence of LED encapsulation: the statistical directivity pattern must represent the LED optics. Normalization can be done using optical axis, then the influence of the artifacts distorting the peak directivity is reduced. Peak normalization was chosen because of its simplicity.

Then all LEDs' diagrams in a batch were averaged. The resulting normalized mean FFP was used in further investigation as the ideal approximation. Refer to Fig. 4 for ideal approximation graphs of all analyzed LEDs.

Results of measured Z2BH FFPs fitting with candidate functions is presented in Fig. 5. The mean FFP is labeled as "ideal" in Fig. 5.

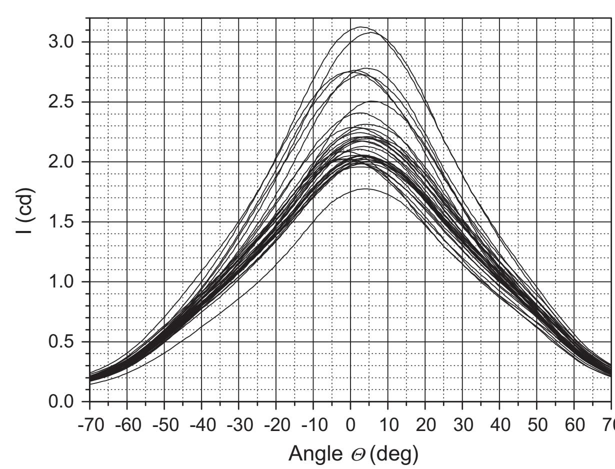

Fig. 2. Measured Z2BH FFPs before normalization.

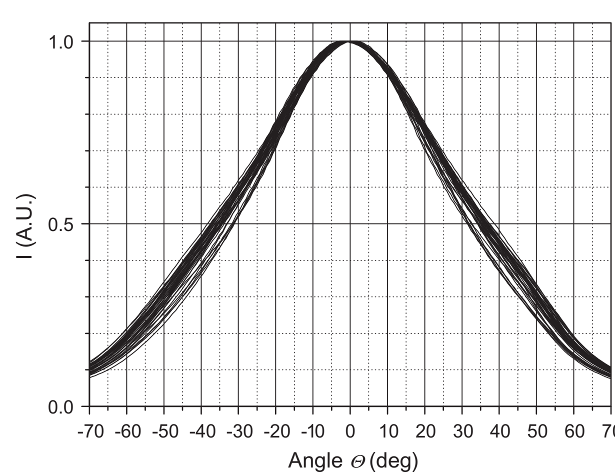

Fig. 3. Measured Z2BH FFPs after normalization.

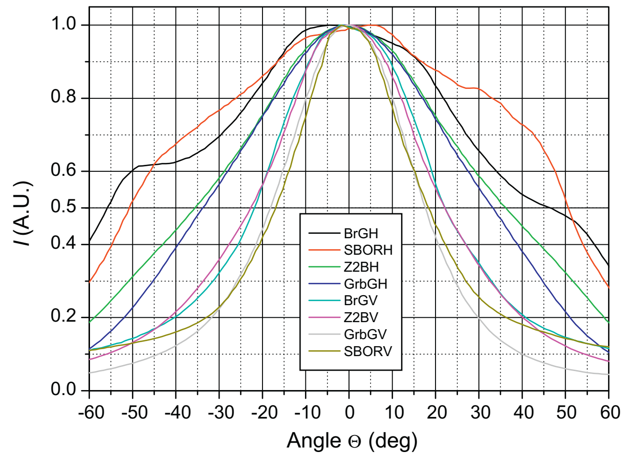

Fig. 4. "Ideal" approximation of LED FFP.

The peak, half power, low and high intensity areas of FFP can be distinguished in Fig. 5.

The "ideal" approximation was used for fitting, but approximation errors analysis was done on every individual LED FFP.

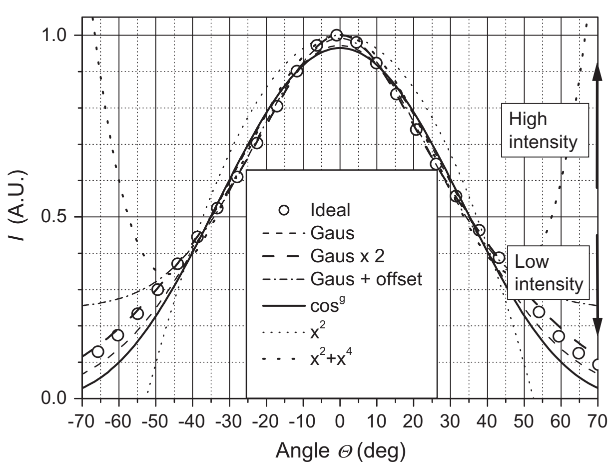

Fig. 5. Measured Z2BH LED FFP approximation by candidate functions.

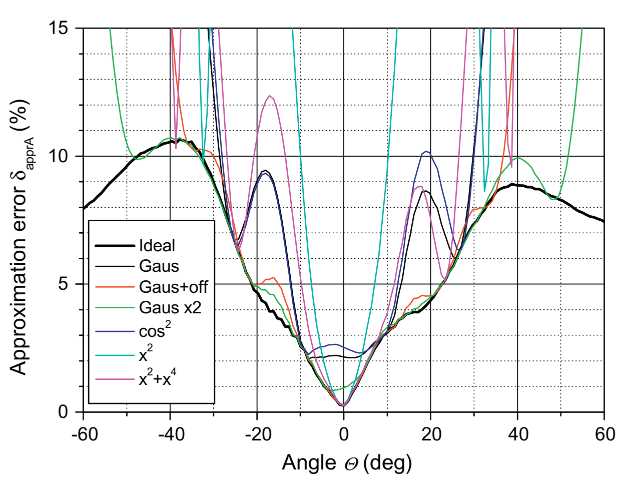

Fig. 6. Intensity approximation error RMS value versus angle (Z2BH LED).

6.2. Error estimates

As an initial investigation, the absolute intensity approximation error at every ith angle was normalized by intensity value has been obtained for every jth LED in a batch and a resulting RMS value calculated (Fig. 6):

$$\delta_{apprA\ i} = \sqrt{\frac{\sum_{j=1}^{M}\left(\frac{I_{orig\ i,j}-I_{appr}(\Theta_{i,j})}{I_{orig\ i,j}}\right)^2}{M}}\cdot 100\%, \tag{14}$$

where index *appr* is used to denote the approximation type ("ideal", "Gaus", "Gaus + offset", etc.) and the *orig* index is for the original (measured) data; letter "*A*" indicates that error variability is analyzed in angle domain.

It can be clearly seen in Fig. 6 that such approximation error increase with angle even for ideal approximation (thick curve). We assumed that best approximation accuracy was desired in high intensity region, at low polar angles. Then the absolute intensity approximation error RMS sum for the particular jth LED can be normalized by sum of N intensity values in FFP:

$$\delta_{apprB\ j} = \frac{\sqrt{\sum_{i=1}^{N}(I_{orig\ i,j} - I_{appr}(\Theta_{i,j}))^2}}{\sqrt{\sum_{i=1}^{N}(I_{orig\ i,j})^2}}\cdot 100\%, \tag{15}$$

where letter "*B*" indicates that analysis is along batch numbers. This relative value of the intensity approximation error RMS was used as the correspondence criterion. If error is normalized in such way then errors at high intensities will have larger influence. The FFP approximation relative errors (Eq. (15)) of individual LEDs were combined by taking the RMS value of errors $\delta_{apprB\ j}$ of M LEDs in a batch:

$$\delta_{appr} = \sqrt{\frac{1}{M}\sum_{j=1}^{M}(\delta_{apprB\ j})^2}. \tag{16}$$

The approximation errors for ideal and investigated function can be used to obtain their cross correlation coefficient:

$$Xcorr_{Err} = \frac{\sum_{j=1}^{M}(\delta_{apprB\ j}\cdot\delta_{idealB\ j})}{\sqrt{\sum_{j=1}^{M}(\delta_{apprB\ j})^2\cdot\sum_{j=1}^{M}(\delta_{idealB\ j})^2}}, \tag{17}$$

where $\delta_{apprB\ j}$ is the relative intensity approximation RMS error of jth LED using one of the candidate function ("appr" = "Gaus", "Gaus + offset", etc.) and $\delta_{idealB\ j}$ is the relative intensity approximation RMS

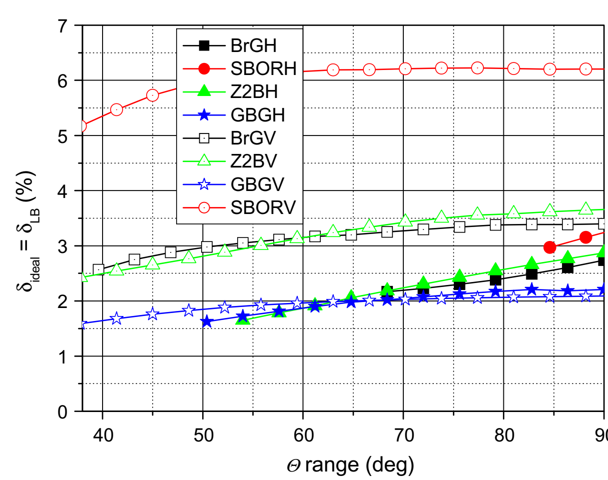

Fig. 7. Intensity variation from ideal approximation within batch is suggested as a lower error bound.

error of jth LED in a batch for "ideal" (mean) approximation. The use of cross correlation coefficient should allow tracing the covariance of the candidate function and the "ideal" approximation errors: values above 0.7 should indicate the similar errors and values below would indicate that errors are significant and candidate function is not following the ideal approximation.

6.3. Lower error bound

In case of "ideal" approximation the errors obtained can be considered as lower error bound. The range used for approximation was varied from slightly below $2\Theta_{0.5}$ to ~180°. Range was placed symmetrically around the peak. Results for "ideal" approximation are presented in Fig. 7.

Relative intensity approximation error (Eq. (16)) was calculated for every range. Then it was assumed that lower error bound should be defined by variance within a batch: the obtained relative intensity approximation error RMS values were treated as lower error bound ($\delta_{LB} = \delta_{ideal}$) in the following analysis.

6.4. Desired range estimation

The estimation of desired range was based on the target application for LEDs used in analysis: large scale video displays. When viewing a LED video display, the human eye is gathering light not from a single LED, but from a given area of the display. Observing the display at sharper angle, this area actually increases. This

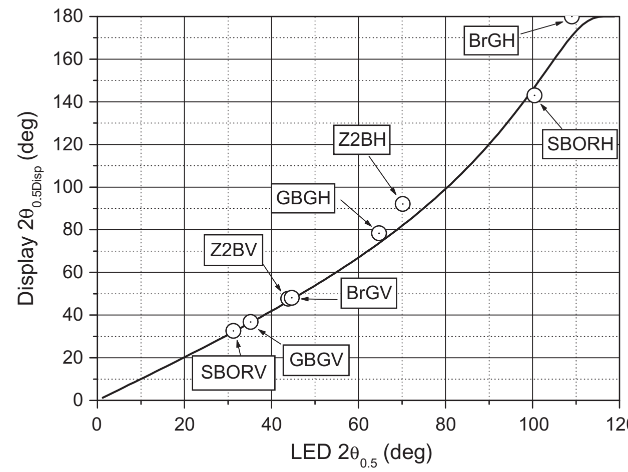

Fig. 8. Display viewing angle relation to half power angle $2\Theta_{0.5}$ (circles–measurement data).

effect will modify the display luminance by cosine law. Therefore screen luminance $Y_{SC}(\Theta)$ spatial distribution along observation angle Θ can be calculated as:

$$Y_{Disp}(\Theta) = \frac{I(\Theta)}{\cos(\Theta)}. \tag{18}$$

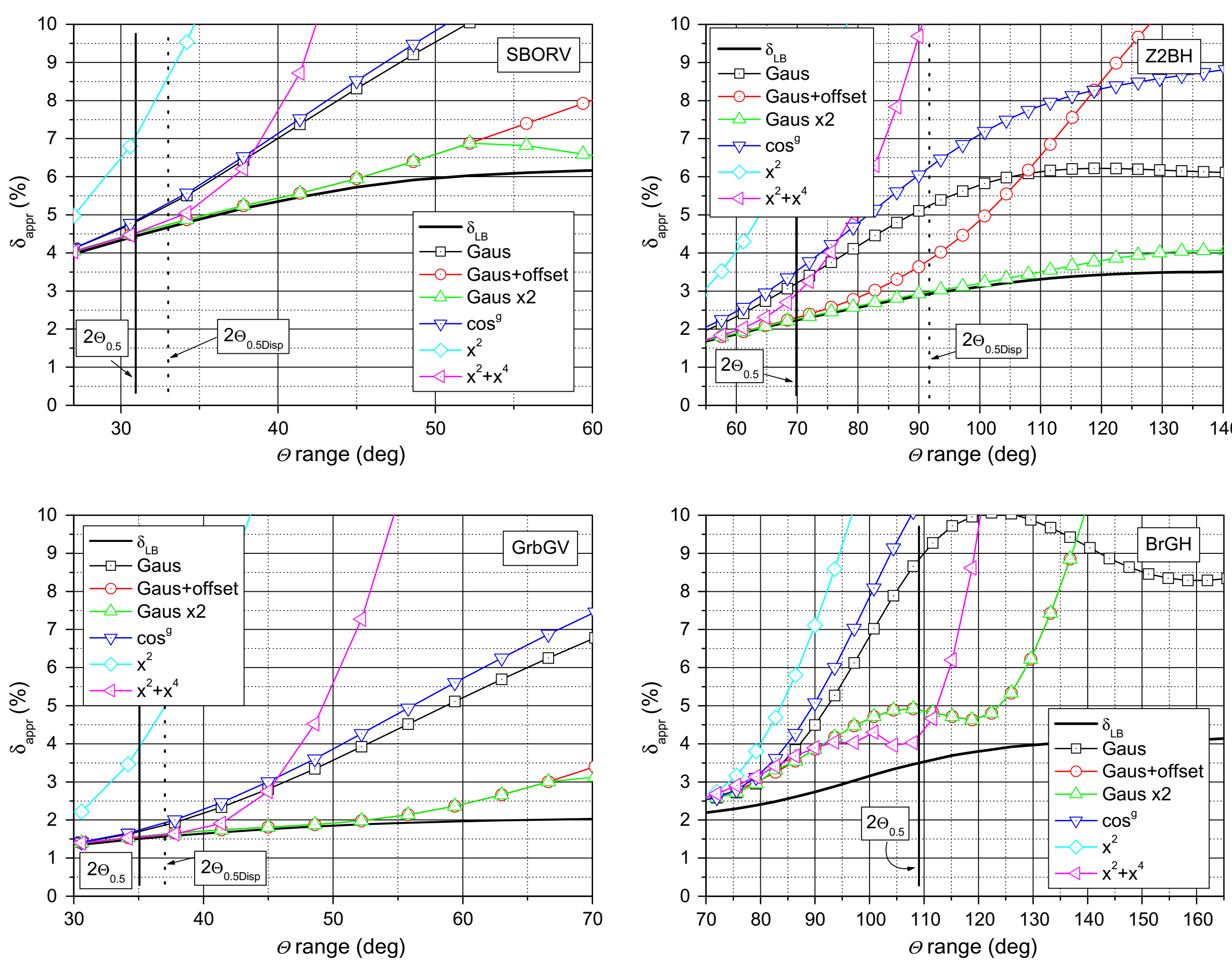

Fig. 9. Relative intensity approximation RMS error versus range.

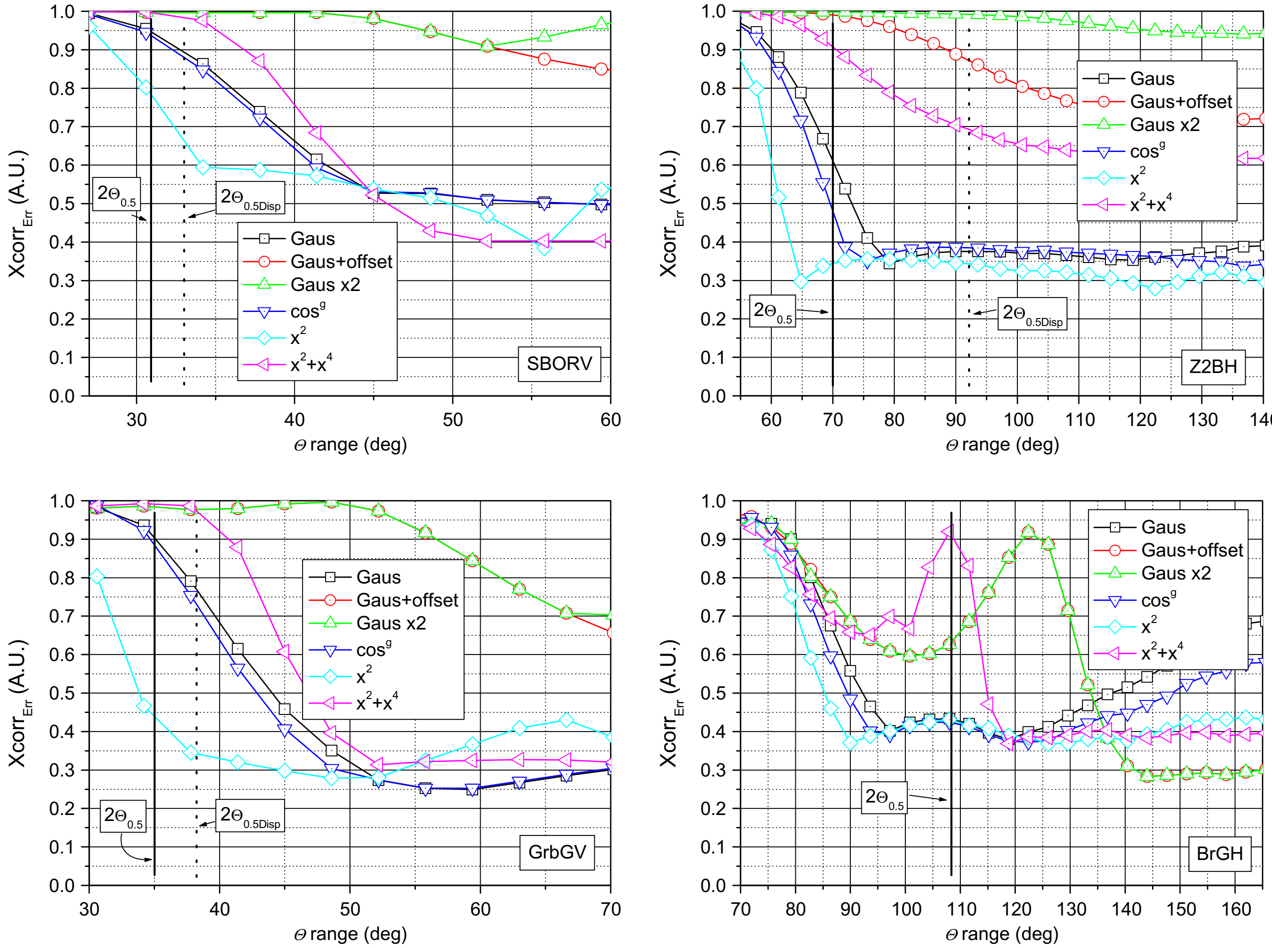

Fig. 10. Approximation errors cross correlation (ideal to candidate) versus range.

The Eq. (15) was applied on measured average FFP and resulting display luminance directivity function was used to obtain the display half power (viewing) angle $2\Theta_{0.5Disp}$. If Eq. (5) can be used to approximate the LED FFP, then display luminance directivity function can be easily obtained from (18) as:

$$Y_{Disp}(\Theta) = I_{\max} \cdot \cos(\Theta)^{g-1}, \tag{19}$$

Display viewing angle is defined as angle at which luminance is dropping to the half of its peak value at angle normal to the display surface. Then display viewing angle $2\Theta_{0.5Disp}$ relation to LED half power angle $2\Theta_{0.5}$ can be established

$$2\Theta_{0.5Disp} = 2\arccos\left(\cos(\Theta_{0.5})^{\left(-\frac{\ln(2)}{\ln(2)+\ln(\cos(\Theta_{0.5}))}\right)}\right). \tag{20}$$

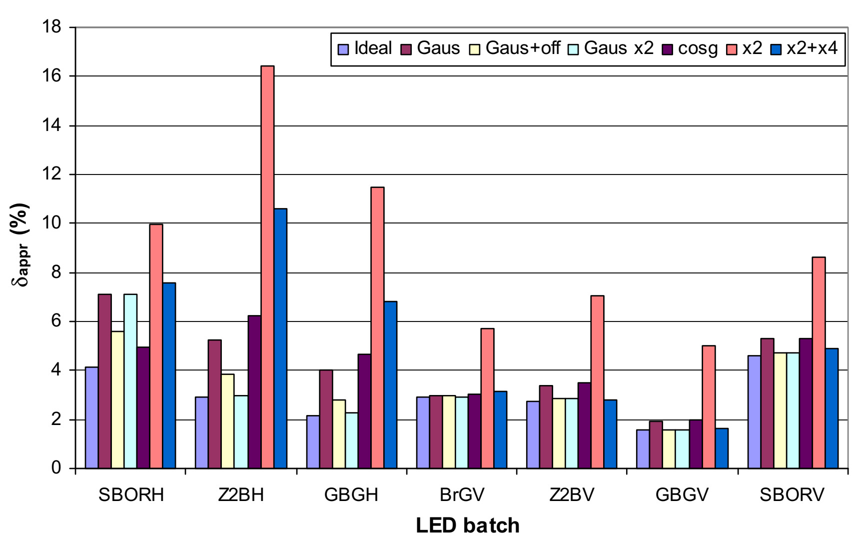

Fig. 11. Relative approximation error (%) RMS value versus LED batch.

The result of display viewing angle calculation based on Eq. (20) and the angles obtained from measurement results based estimation are presented in Fig. 8.

If LED display is designed to assure certain viewing angle $2\Theta_{0.5Disp}$, then display image quality beyond this range is less important. Therefore we assume that accuracy of LED FFP approximation beyond the display viewing angle $2\Theta_{0.5Disp}$ can be lower. The approximation performance study has been carried out in whole $-90^\circ \ldots +90^\circ$ range but later analysis range was reduced range according to Fig. 8.

7. Approximation performance evaluation

Same representative batches (Table 2) have been approximated by all the candidate functions (Table 1). The relative intensity approximation RMS error has been obtained for every LED. The RMS errors of within a batch were combined using two criteria: RMS value (Eq. (16)) and cross correlation coefficient (Eq. (17)).

Graphs representing the error variance are presented in Fig. 9. The reference lines indicating the LED half power angle $2\Theta_{0.5}$ (vertical solid line) and the display viewing angle $2\Theta_{0.5Disp}$ (vertical dashed line) values are added. The most representative results are presented in Fig. 9: from narrow (SBORV) to wide (BrGH) angle FFP.

Analysis indicates that the intensity approximation error is increasing when range is increased. As expected, dual term Gaussian and Gaussian with offset functions have demonstrated the best performance. But the rest of the candidates, except parabolic function, also have acceptable performance within display viewing angle $2\Theta_{0.5Disp}$ range: single term Gaussian and $\cos^g$ function errors are just 20% larger than lower error bound δ_{LB} for the SBORV LED (Fig. 9).

Analysis of relative approximation errors does not indicate direct relation to ideal approximation. Therefore we have introduced the approximation errors of ideal and candidate function correlation (Eq. (17)). In such way we can analyze whether larger errors for current LED in a batch are caused by deviation of individual

Table 3
LED FFP approximation error RMS value.

Notation	Measured $2\Theta_{0.5}$, °	Relative approximation error @ $2\Theta_{0.5Disp}$ range, δ_{Gapr} (%)						
		Ideal	Gaus	Gaus + off	Gaus $x2$	$\cos^g$	x^2	x^2+x^4
SBORH	99.6 ± 3.8	4.14	7.1	5.57	7.08	4.95	9.95	7.56
Z2BH	70.3 ± 3.6	2.89	5.25	3.87	2.98	6.26	16.4	10.6
GBGH	64.7 ± 2.1	2.16	4.03	2.8	2.26	4.67	11.5	6.8
BrGV	44.6 ± 1.9	2.92	3	2.95	2.94	3.05	5.68	3.14
Z2BV	43.9 ± 2.0	2.74	3.38	2.87	2.87	3.5	7.03	2.8
GBGV	35.2 ± 0.9	1.6	1.9	1.6	1.6	2	5	1.62
SBORV	31.3 ± 3.2	4.6	5.3	4.7	4.7	5.3	8.6	4.9

Table 4
LED FFP approximation errors cross correlation.

Notation	Measured $2\Theta_{0.5}$, °	Cross correlation coefficient @ $2\Theta_{0.5Disp}$ range, $Xcorr_{Err}$					
		Gaus	Gaus + off	Gaus $x2$	$\cos^g$	x^2	x^2+x^4
SBORH	99.6 ± 3.8	0.578	0.698	0.578	0.78	0.458	0.555
Z2BH	70.3 ± 3.6	0.375	0.837	0.992	0.387	0.34	0.694
GBGH	64.7 ± 2.1	0.666	0.869	0.982	0.604	0.44	0.335
BrGV	44.6 ± 1.9	0.985	0.995	0.997	0.98	0.63	0.986
Z2BV	43.9 ± 2.0	0.854	0.977	0.997	0.825	0.4	0.997
GBGV	35.2 ± 0.9	0.771	0.977	0.997	0.731	0.34	0.971
SBORV	31.3 ± 3.2	0.895	0.977	0.997	0.88	0.662	0.983

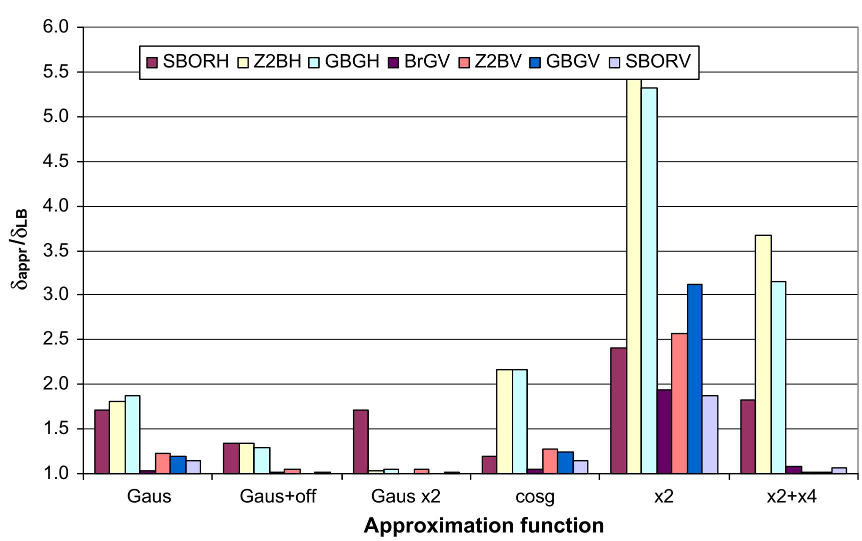

Fig. 12. Relative approximation error RMS value as a fraction of lower error bound versus approximation function.

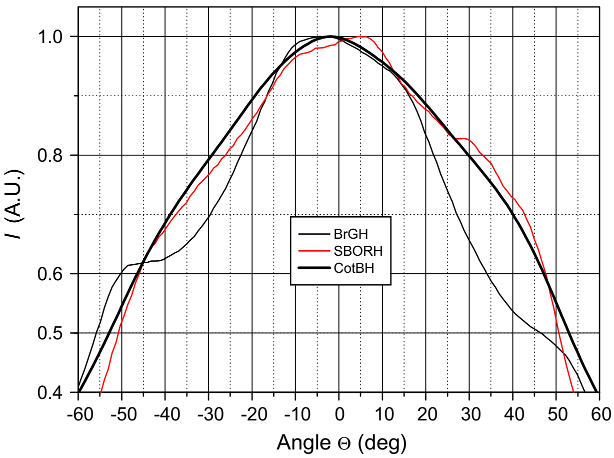

Fig. 13. Comparison of wide angle FFP of high quality LED (CotBH, thick line) and BrGH and SBORH LEDs.

LED FFP from common batch behaviour (ideal approximation – in such case correlation coefficient will be high) or by incapability of approximating function to follow the ideal FFP curvature (in such case correlation coefficient will be low).

Results obtained at display viewing angle $2\Theta_{0.5Disp}$ range are presented in Fig. 11 and Tables 3 and 4. Grouping the results according to LED type is not convenient for analysis. One conclusion can be drawn from Fig. 11: fourth order polynomial approximation is producing large errors for GBGH and Z2BH LEDs (both are 70°). Higher order polynomial was not included in graphs at all: errors are large as it can be seen from Figs. 5, 6, 9 and 10. BrBH data was not included because it is impossible to get reliable results at 180° angle.

Results in Fig. 12 are more convenient for analysis. It can be seen that all Gaussian functions have best performance. Approximation results are worse for wide angled SBORH. This can be explained by more complicated directivity function of wide angle LEDs (refer Fig. 4): aforementioned functions have complex curvature. Modern, high quality LEDs dedicated for professional video displays, like Cotco's Screen Master [20], have much smoother directivity. Refer to Fig. 13 for LO5SMQBL4-B0G (Cotco's Screen Master blue LED) [13] directivity comparison against BrHG and SBORH LEDs.

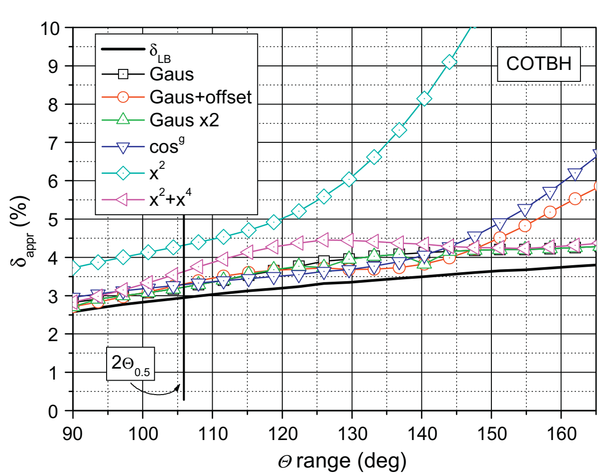

Fig. 14. Cotco's Screen Master's FFP approximation error versus range.

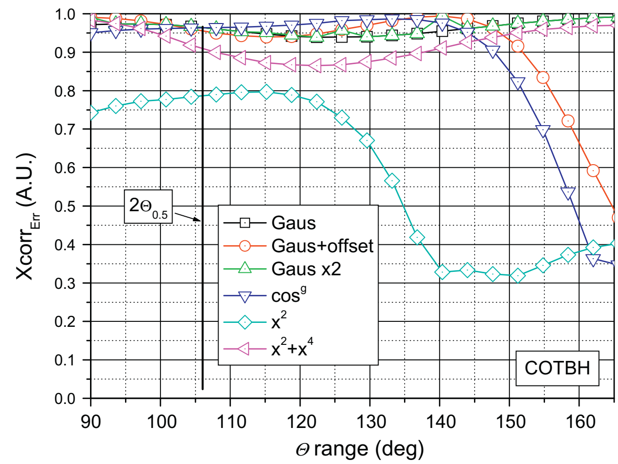

Fig. 15. Approximation errors cross correlation (ideal to candidate) versus range (Cotco's Screen Master).

Same relative approximation errors (Fig. 14) and approximation errors correlation of ideal to candidate functions analysis (Fig. 15) was carried out.

Thanks to Cotco's Screen Master FFP smoothness the approximation performs better even for such simple functions like single term Gaussian and raised cosine: relative approximation error at half power beam angle $2\Theta_{0.5}$ is close to lower error bound and errors correlation is above 0.7.

We conclude that application of suitable higher order/larger terms number function for approximation can get close to lower error bound. In our case it was dual term Gaussian function. But for general engineering tasks it should be sufficient to have 5–8% relative approximation error or close to twice the lower error bound. In such case even simple, single term functions have satisfactory performance. We name the Gaussian without DC offset as best candidate. Then such simple function can be used to approximate the directivity only having the vertical and horizontal half power beam angle $2\Theta_{0.5}$ available from manufacturer data sheet: this angle is already included in Eq. (7).

8. Conclusions

Investigation indicates that approximation function such as dual term Gaussian can produce the results that are close to ideal approximation. However, even simple, single term functions have 5–8% relative approximation error and are below double lower error bound in reduced angular range, corresponding to display half radiance angle. We consider such performance as satisfying for general engineering tasks like illumination rendering or display directivity performance prediction.

References

[1] F. Nguyen, Challenges in the design of a RGB LED display for indoor applications, Synthetic Metals 122 (2001) 215–219.
[2] P.H. Putman, LED displays: light up the big screen, Sound and Video Contractor (2000).
[3] D. Vazquez-Molini et al., Louvers design for LED displays for sunny days, Displays 28 (2007) 167–173.
[4] L. Svilainis, V. Dumbrava, Estimation of the louvers influence on LED video display image visibility, in: Proceedings IEEE ITI'09, Croatia, 2009, pp. 571–576.
[5] B. Wendler, LED Viewing Angles vs. LED Video Display Viewing Angles, Technical Note 40, Daktronics Inc., USA, 2002.
[6] I. Moreno, U. Contreras, Color distribution from multicolor LED arrays, Optics Express 15 (6) (2007) 3607–3618.
[7] The Radiometry of Light Emitting Diodes, Labsphere Inc., UK, 2001.

[8] W.J. Cassarly, LED Modelling: Pros and Cons of Common Methods, Photon, Tech Briefs IIa-2a, Special Supplement to NASA Tech Briefs, April 2002.
[9] I. Moreno, C.C. Sun, Modelling the radiation pattern of LEDs, Optics Express 16 (2008) 1808–1819.
[10] I. Moreno et al., Simple function for intensity distribution from LEDs, Proceedings of SPIE 6670 (2007) 66700H1-7.
[11] R. Young, LED measurement instrumentation, CIE Advanced LED Seminar, 2001.
[12] A.A. Gaertner, LED Measurement Issues, Institute for National Measurement Standards Canada NRC, April 2002.
[13] Specification for Cotco 110 Degree Oval LED Lamp in Blue Color with Tinted Diffused Lens and Stopper, Model No.: LO5SMQBL4-B0G, Doc. No.: B 24 November 2003, Cotco International Ltd., 2002.
[14] D. Barton, Radar Technology Encyclopedia, Artech House Inc., Norwood, 1998.
[15] L. Svilainis, V. Dumbrava, LED far field pattern approximation performance study, in: Proceedings IEEE ITI'07, vol. 29, Croatia, 2007, pp. 645–649.
[16] H. Yang, J.W.M. Bergmans, T.C.W. Schenk, J.M.G. Linnartz, R. Rietman, Uniform illumination rendering using an array of LEDs: a signal processing perspective, IEEE Transactions on Signal Processing 57 (3) (2009) 1044–1057.
[17] L. Svilainis, LED directivity measurement in situ, Measurement 41 (6) (2008) 647–654.
[18] J.A. Nelder, R. Mead, A simplex method for function minimization, Computer Journal 7 (1965) 308–313.
[19] L. Svilainis, V. Dumbrava, LED goniometry system, Electronics and Electrical Engineering 72 (8) (2006) 69–74.
[20] Cotco "Next Generation" Screen Master LEDs, Marktech Optotelectronics, 2010. <http://www.marktechopto.com/About-Marktech/press-details.cfm?NewsID=13>.